Infra-red spectroscopic characterization of the $\alpha \rightarrow \beta$ phase transition in poly(tetramethylene terephthalate)

P. C. Gillette*, J. B. Lando and J. L. Koenig
Department of Macromolecular Science, Case Western Reserve University, Cleveland, Ohio 44106, USA
(Received 29 January 1984; revised 16 March 1984)

The mechanically induced crystal:crystal phase transition observed in poly(tetramethylene terephthalate) PTMT has been characterized using simultaneous stress, strain, and infrared measurements. Infrared data indicate that after the first deformation cycle the transition is reversible. Interconversion from α to β starts at a strain of 5% with the relative concentration of the 2 crystal phases in proportion to the applied strain up to 20%. Factor analysis of spectra collected over the course of a single deformation cycle indicates that the amorphous phase is not converted to either of the crystal phases.

(Keywords: PTMT; PBT; phase transitions; *FT*i.r.; mechanical properties)

INTRODUCTION

Although a number of polymers possess several distinct crystal forms, poly(tetramethylene terephthalate) (PTMT or PBT) is especially intriguing from a scientific standpoint because of the mechanism of the phase transition. The application of uniaxial stress has been found to induce a reversible crystal:crystal phase transition[1]. Attempts to characterize the transition utilizing a wide variety of methods have generated conflicting results.

It is interesting to note that there exist a number of different crystal structures in the poly(*m*-methylene terephthalate) series. Poly(ethylene terephthalate) has the well known crystal structure involving *trans* methylenes. Poly(trimethylene terephthalate), however, has been shown[2,3] to crystallize in a T–G–G–T conformation. Three different structures have been observed for poly(hexamethylene terephthalate)[4], although all possess aliphatic residues in extended conformations with the major differences among the structures lying in chain packing. Other polymers which exhibit stress induced crystal:crystal phase transitions[5] include: poly(β-propiolactone), polypivalolactone, poly(α-methyl-α-n-propyl-β-propiolactone), poly(α-methyl-α-ethyl-β-propiolactone), poly(β-hydroxybutyrate), and poly(α-α-diethyl-β-propiolactone), although annealing is required in all cases to recover the unstressed crystal phase.

X-ray investigations of PTMT have produced conflicting results[6-16]. An overview of the crystallographic work on the 2 crystal phases is presented in refs. 10 and 12. The major distinctions between the α and β phases have been found to lie in the conformation of the flexible tetramethylene segment of the molecule. In the unstressed form the aliphatic residue assumes a crumpled conformation (A–T–A) (where A = non*trans*:non*gauche*, T = *trans*) which is converted to the extended moiety (T–T–T) upon the application of stress[6-10,15]. Fibre patterns must be corrected for the fact that there exists a tilt of the molecular axis with respect to fibre axis[8]. It is the nature of the bond rotation angles in the two forms which has generated the greatest debate.

Recent n.m.r. results have provided some insight into structures associated with the 2 crystal phases. On the basis of broad line n.m.r. measurements Davidson *et al.*[17] concluded that the aliphatic segment is, in fact, extended in a sample under stress and is best represented by the model of Hall and Pass[9]. Their results suggest, however, that the conformation of the central methylene pairs does not change substantially in the transition which is not in agreement with any of the published structures for the α crystal phase.

Jelinski *et al.*[17-22] have utilized solid state ^2H and ^{13}C n.m.r. to investigate a wide range of PBT copolymers and model compounds. Relaxation data[21] and chemical shift anisotropy considerations indicate that the motions of the terephthalate groups are relatively slow in comparison to the aliphatic segment. Selectively deuterated compounds[20] have provided insight into the kinds of motions present. A wide range of motions have been postulated, but n.m.r. data indicate that most favoured motions are concentrated in the central methylene groups with no large scale reorientation of the OCH_2 carbons.

Infra-red spectroscopic investigations[23-37] have detected a number of conformationally sensitive bands. The greatest changes are found to occur in the methylene rocking region[23], although C–H bending modes also exhibit good sensitivity. Ward and Wilding[23] reported the first infra-red spectroscopic investigation of the 2 crystal forms in which they made a number of band assignments. Additional studies by Stambaugh *et al.*[25,30] provided more detailed information concerning spectral changes as a function of a wide variety of sample treatments. Using the force constants from a normal coordinate analysis

* Present address: Hercules Research Center, Lancaster and Hercules Roads, Wilmington, Delaware, USA

0032-3861/85/020235-06$03.00

(NCA) of PET[38] as a starting model, Stach[34] has recently completed NCA calculations for both crystal conformations (preliminary results of this work are presented in ref. 31).

A number of techniques have been utilized to monitor the crystal:crystal phase transition. Jakeways *et al.*[39,40] reported observing changes in both the position and intensity of the $\langle \bar{1}04 \rangle$ and $\langle \bar{1}06 \rangle$ reflections at strain levels as low as 4%. With the use of a position sensitive detector (PSD), Alter and Bonart[41] detected the onset of the transition to occur at a strain of 6% with full conversion of $\alpha \rightarrow \beta$ at 15%. Raman investigations[39,40] reveal differences in the intensity of the 888 cm^{-1} mode. Both the X-ray and Raman work must be viewed with some reservation, however, since in both instances the times required for the measurements were relatively long (with the exception of X-ray measurements made with a PSD). Nevertheless, the work was successful in demonstrating the reversibility of the phase transition. The results of small angle X-ray diffraction[41] indicate that the long period increases roughly in proportion to the strain, although at a strain corresponding to ~5% (an inflection point is observed in the stress:strain diagram at this point) it increases more rapidly.

Recent dynamic (fast scan) Fourier transform infra-red work[24,26-29,34,37] has permitted the characterization of this transition on a much shorter time scale than has been possible with either conventional infra-red, Raman, or X-ray diffraction. This technique has detected the onset of the phase transition at strain levels of 2%. Siesler has reported[28], however, that the transition is not fully reversible since the intensities of conformationally sensitive modes do not revert to their original unstressed values upon relieving stress.

Simultaneous *FT*i.r. and mechanical property measurements afford a unique opportunity to obtain molecular information concerning a macroscopic deformation. In principle *FT*i.r. represents the ideal technique to monitor conformational changes since information may be obtained regarding both crystalline and amorphous regions on a very short time scale. (It should be remembered, however, that infra-red measurements cannot necessarily distinguish between molecules in the crystal and amorphous domains having the same conformation.) Several factors, however, complicate spectral analysis in such experiments. Interpretation of spectroscopic changes is hampered by the fact that the most sensitive modes are extensively overlapped making quantitative measurements extremely difficult. Due to the copious quantities of information generated by these experiments (e.g. a typical i.r. experiment results in 100 spectra each containing 1500 absorbance values), it has been necessary to develop a wide range of computer programs to facilitate spectral data processing. Given the recent progress in the area of spectroscopic data processing, it was thought that considerably more information could be extracted from the spectra than has been possible previously.

EXPERIMENTAL

In order to measure infra-red spectra, stress and strain simultaneously, the apparatus in *Figure 1* was constructed with the help of the departmental technician, Alex Schnitlinger. The key instruments involved are a DIGILAB FTS20-E Fourier transform infra-red spectrometer

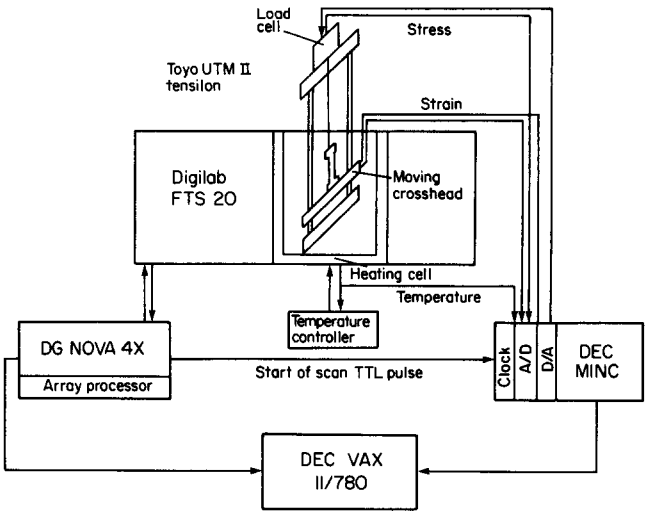

Figure 1 Schematic of apparatus used to make simultaneous stress, strain and *FT*i.r. measurements

equipped with a mercury cadmium telluride (MCT) detector (mirror velocity = 1.2 cm s^{-1}) and a Toyo UTM-II tensilon. Rather than attempting to incorporate the necessary hardware to monitor mechanical properties variables into the *FT*i.r. Data General NOVA 4X computer, it was decided to take advantage of a DEC MINC computer already owned by the department. This not only resulted in substantial monetary savings, but it would have been fairly difficult to incorporate the necessary software within the program which collects spectra (IMX).

To synchronize measurements, a TTL level pulse was sent by the *FT*i.r. (via the IMX command PUL) each time a spectrum was collected. This pulse served as the input to a Schmitt trigger located on the MINC clock module which initiated sampling of the appropriate signals. Linear potentiometers were used in conjunction with 12-bit A/D converters to monitor stress and strain, which were driven by reference voltages supplied by D/A converters on the MINC. By applying a reference voltage of 10.24 volts on the strain potentiometer, and digitizing ± 5.12 volts in 4096 increments, the digitization limit for strain is 40 μm.

To investigate the reversibility of the $\alpha \rightarrow \beta$ transition, a 'dog-bone' shaped 40 μm film sample of PTMT (17 mm × 45 mm) (BASF Ultradur 4500 supplied by Prof. K. Holland-Moritz of Universität Köln) was drawn to 275% of its initial length on an Instron at a rate of 10 mm min^{-1}. It was then annealed (not under tension) at a temperature of 150°C under vacuum for 9 h, and allowed to slowly cool to room temperature. This treatment was designed to produce an oriented sample with high degree of α crystallinity which was confirmed by infra-red dichroic measurements.

The specimen was then cut to dimensions of 11 × 18 mm and subjected to a 'sawtooth' strain function with a maximum strain of 20% for 5 cycles at a rate of 0.4 mm min^{-1}. All spectra were collected coadding 10 scans each of sample and reference with a 3 mm aperture, undersampling factor = 4 to conserve both disc space and computation time, nominal resolution of 4 cm^{-1}, and Fourier transformed after zero filling to double the initial interferogram file size. A plot of the resulting stress:strain cycle (*Figure 2*) reveals that some irreversible changes

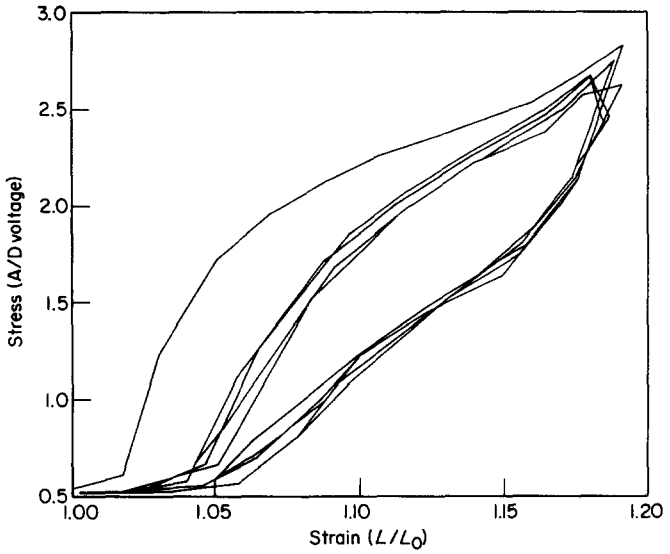

Figure 2 Stress voltage as a function of strain for cycling experiment

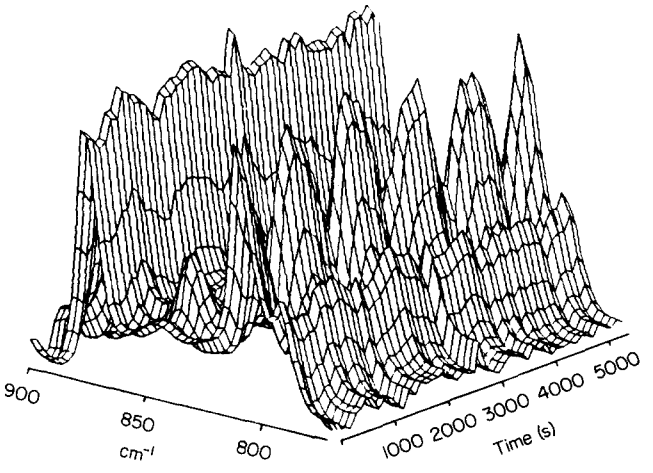

Figure 3 Surface plot of absorbance as a function of time in the region 900–775 cm^{-1} after compensating for changes in sample thickness

occur during the first cycle. After the first cycle, however, the sample appears to deform in a completely reversible fashion.

INFRA-RED ANALYSIS

Changes in sample thickness over the course of the experiment were compensated for by scaling all spectra by a factor corresponding to the applied strain. Scale factors computed in this fashion were in close agreement with those computed by using the integrated intensity of the 1505 cm^{-1} ring mode. The use of a common scale factor for the entire spectral region indicates that the spectral changes cannot be due to further induced orientation. Therefore, the spectroscopic changes are molecular in nature rather than orientational.

900–740 cm^{-1} region

In this region of the spectrum a number of conformationally sensitive modes appear as shown by *Figure 3* which possess highly coupled potential energy distributions. The region is characterized by 5 dominant peaks appearing at 874, 845, 811, 796 and 750 cm^{-1}. Not surprisingly the 874 cm^{-1} ring C–H out of plane deformation mode remains essentially constant over the course of the experiment. The relative changes in integrated absorbance intensity for the conformationally sensitive 811, 845 and 796 cm^{-1} peaks are plotted in *Figure 4*. (Relative values were computed by scaling the areas corresponding to each peak to the maximum area for that peak over the course of the experiment.) A weak band appearing at 845 cm^{-1} the unstrained sample is seen to greatly increase in intensity with increasing strain which is accompanied by a corresponding decrease in intensity in the 811 cm^{-1} peak. Both of these modes contain rocking motions of the methylene groups found in the α and β crystal phases respectively. A small decrease is apparent in the 796 cm^{-1} band with increasing strain.

Methylene rock:wag region (1000–900 cm^{-1})

This region of the spectrum is characterized by 4 dominant peaks appearing at 916, 936, 963 and 989 cm^{-1}. NCA calculations[31,34] and model compound studies indicate that the 916 cm^{-1} band arises primarily from a torsional mode about the C–O–C–C bond observed only in the α conformation. The 963 cm^{-1} mode has a similar potential energy distribution to the 916 cm^{-1} peak, but is observed in the β phase.

Three dimensional plots of the absorbance as a function of (time, cm^{-1}) (*Figure 5*) for this region indicate that a number of spectroscopic changes occur. Band shape analysis of the spectra permits the underlying peaks to be well resolved in terms of 4 Lorentzian band profiles. Plots of integrated intensity of the resolved bands (*Figure 6*) indicate that the 916, 936 and 989 cm^{-1} modes are inversely proportional to the applied stress:strain. The 916 cm^{-1} peak exhibits the greatest sensitivity to stress with its integrated intensity decreasing to less than 20% of the initial area at $\lambda = 1.20$.

The integrated intensity of the 963 cm^{-1} band (*Figure 7*), however, exhibits rather strange behaviour in view of its obvious increase in intensity apparent in the surface plots. NCA calculations indicate that this mode has a potential energy distribution corresponding to coupled O–C stretch, C–O–C and O–C–C bending motions. Closer examination of changes in half width at half height (HWHH) and maximum intensity reveal opposing pheno-

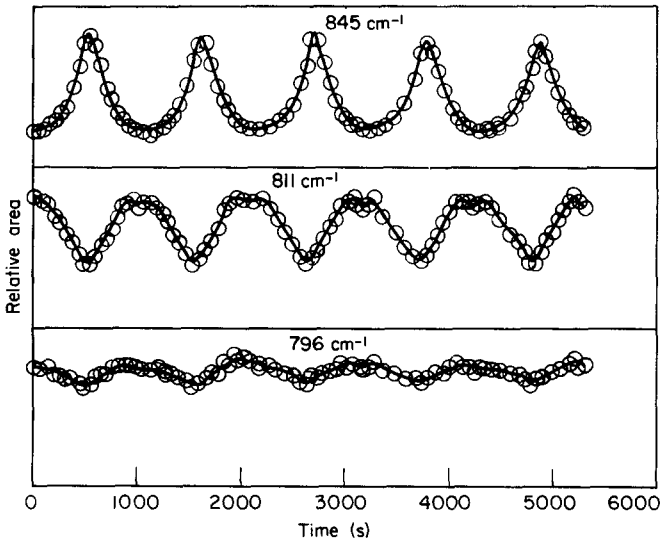

Figure 4 Relative integrated absorbances of 845, 811, and 796 cm^{-1} bands as a function of time

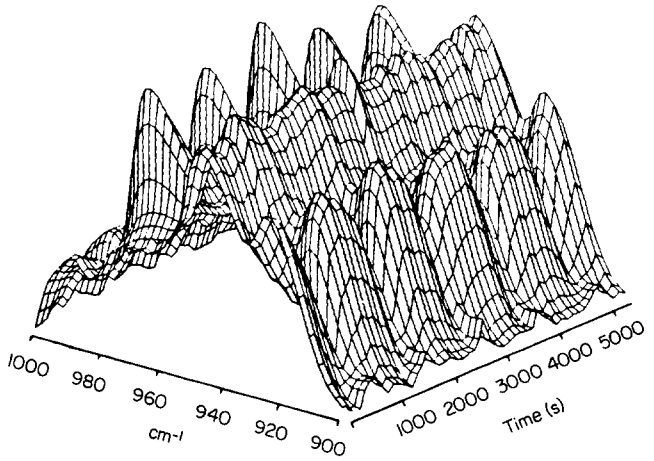

Figure 5 Surface plot of absorbance as a function of time in the region 1000–900 cm^{-1} after compensating for changes in sample thickness

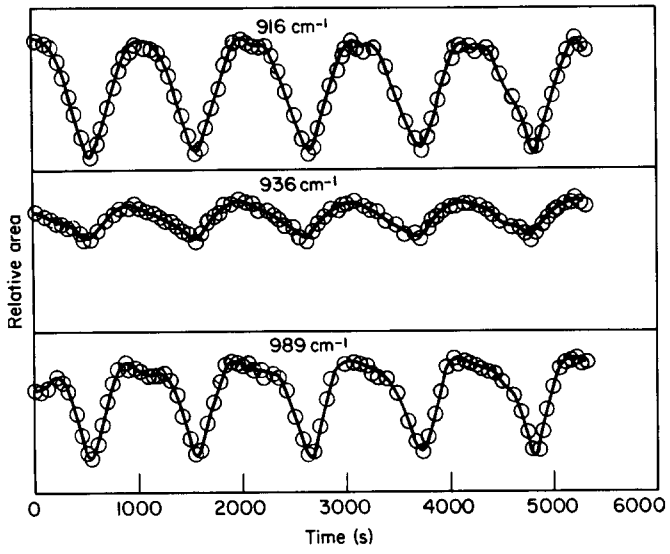

Figure 6 Relative integrated absorbance of 989, 936 and 916 cm^{-1} bands as a function of time

mena. The maximum intensity increases with increasing stress:strain as one would anticipate for a mode characteristic of the β phase, whereas the HWHH decreases. This can be interpreted in terms of a narrowing of the distribution of conformations as the degree of β crystallinity increases.

Methylene bending region (1495–1440 cm^{-1})

Samples of PTMT in this region (*Figure 8*) of the infra-red spectrum are characterized by 4 dominant peaks occurring at 1485, 1470, 1460 and 1450 cm^{-1}. Extensive band overlap of these modes coupled with underlying peaks associated with the amorphous phase does not permit resolution of individual peaks using band shape analysis. Nevertheless it is possible to draw some qualitative conclusions. The 1485 cm^{-1} modes are seen to increase in intensity in proportion with the applied strain and as such are representative of the β phase. There is a corresponding decrease in the 1460 and 1450 cm^{-1} modes with increasing strain confirming these peaks are characteristic of the α phase.

Although a wide range of changes are observed in the infra-red spectra acquired at various points during the deformation cycle, the presence of extensive band overlap precludes drawing any conclusions regarding the exact nature of transition based simply upon inspection. To a first order approximation, samples can be thought of as consisting of 3 distinct phases: α, β and amorphous. In order to assess the role of the 3 phases in the transition it is critical to determine how many components are spectroscopically identifiable. To this end, factor analysis of the spectra should provide the appropriate information.

To preserve the statistically random error and maintain the spectral reference point of 0 absorbance units, factor analyses were carried out on the original (i.e. unscaled) spectra using covariance about the origin. Calculations were initially performed on the 1000–900 cm^{-1} region using 20 spectra collected during the second strain:relax cycle. A linear baseline correction was applied to all files prior to processing. A plot of log(λ) *versus* number of components (*Figure 9*) suggests that there exist 2 pure components. The real error (*Figure 10*) drops to 0.3 units at 2 components which is in the range of error anticipated for these data. Similarly the cumulative per cent variance (*Figure 11*) of the 2 primary eigenvalues accounts for 99.99% of the total variance. These results imply that the

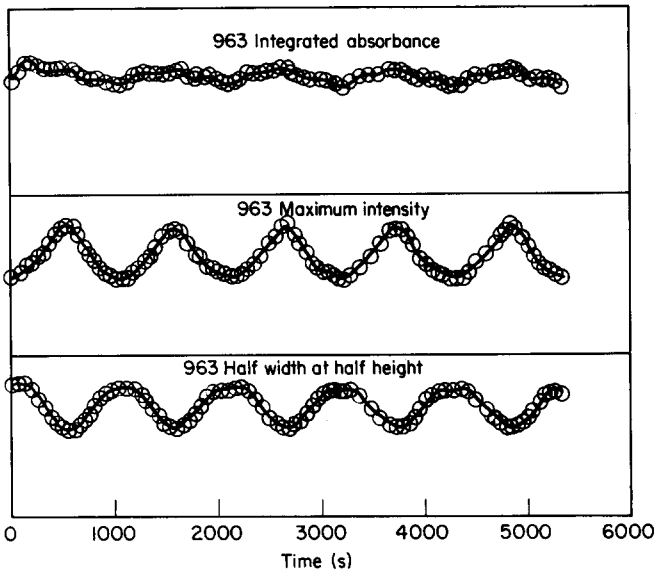

Figure 7 Relative integrated absorbance, half width at half height, and maximum intensity of 963 cm^{-1} band as a function of time

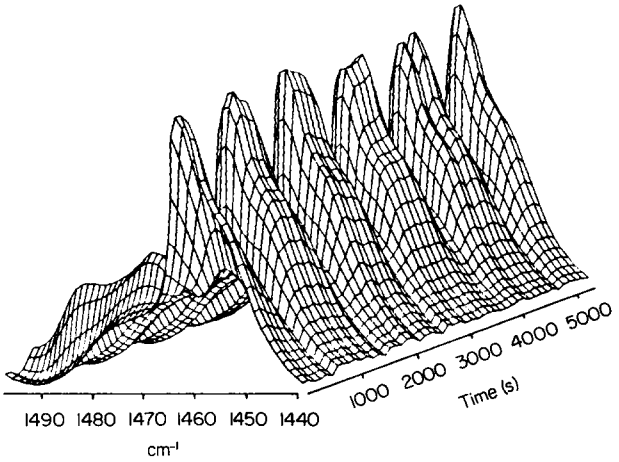

Figure 8 Surface plot of absorbance as a function of time in the region 1495–1440 cm^{-1} after compensating for changes in sample thickness

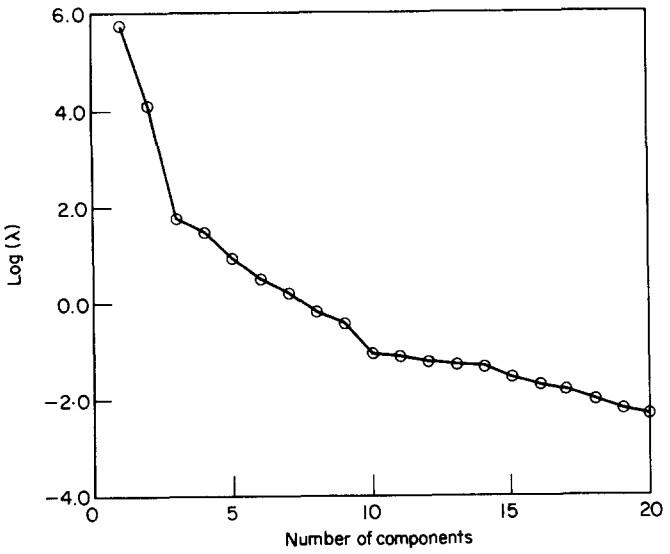

Figure 9 Log (λ) plot for factor analysis using 20 spectra collected during second cycle based on the region 1000–900 cm^{-1}

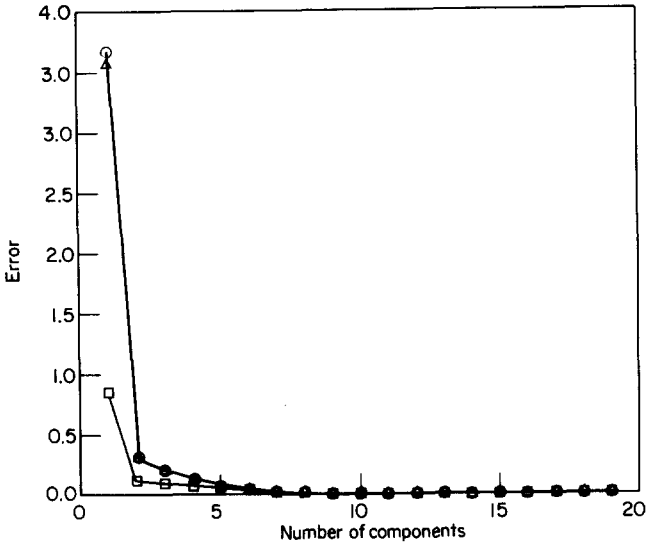

Figure 10 Real, extracted, and imbedded error functions for factor analysis using 20 spectra collected during second cycle based on the region 1000–900 cm^{-1}. (○) Real error; (×) imbedded error; (△) extracted error

spectroscopic data can be modelled as a 2 component system. Siesler has noted[28] the presence of an isosbestic point at 1466 cm^{-1} which implies a conversion of one modification to another without a third being formed. To confirm the preceding conclusion another calculation was carried out using the region 1490–1440 cm^{-1} since it has been suggested[31] that this portion of the spectrum is sensitive to conversion of the amorphous phase to β crystallinity which produced similar results concerning the number of pure components.

Factor analysis clearly demonstrates that 2 principal components are involved in the transition. Since X-ray measurements have shown that the α phase is converted to the β form, the amorphous phase is not transformed into either α or β since the spectra of the 2 crystal phases must correspond to the pure components. This is not to say that there are not conformational changes in the amorphous phase during the deformation. The type of changes occurring in the amorphous phase cannot necessarily be detected by these infra-red measurements.

Given the fact that spectroscopic changes arise from the crystal:crystal phase transition, it is relatively simple to determine the relative amounts of α and β present at each point in the experiment by selecting 2 spectra at the extreminities of the deformation cycle to define 'pure' α and β crystallinity. The least squares scaling coefficients based on a fit of these 2 spectra to each spectrum collected during the deformation cycles will be directly proportional to the actual concentrations of the 2 crystal phases. A plot of the relative crystallinity as a function of strain (*Figure 12*) suggests that the conversion of α to β is a linear function of strain above ~5%, although there appears to be some hysteresis evident. These data clearly illustrate the reversibility of the transition for calculations based on the 1000–900 cm^{-1} region of the spectra. This could arise from minute spectroscopic variations detected in the amorphous phase, or orientation effects. The relationship between the 2 crystal phases and observed stress (*Figure 13*), on the other hand, appears to be far more complex.

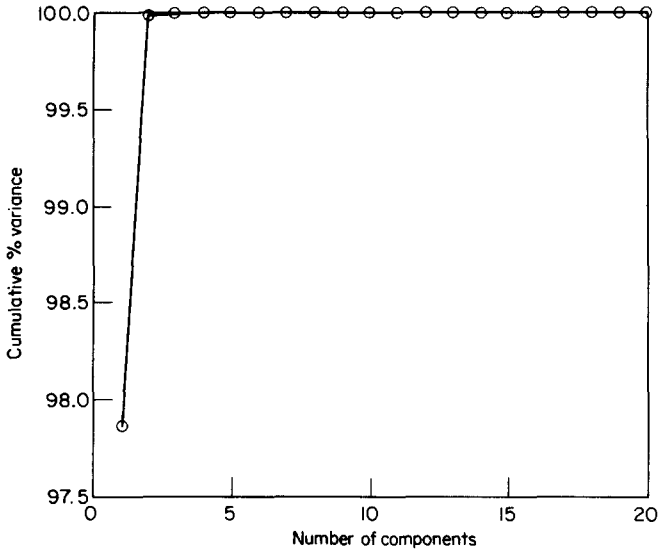

Figure 11 Cumulative % variance as a function of number of pure components for factor analysis using 20 spectra collected during second cycle using based on the region 1000–900 cm^{-1}

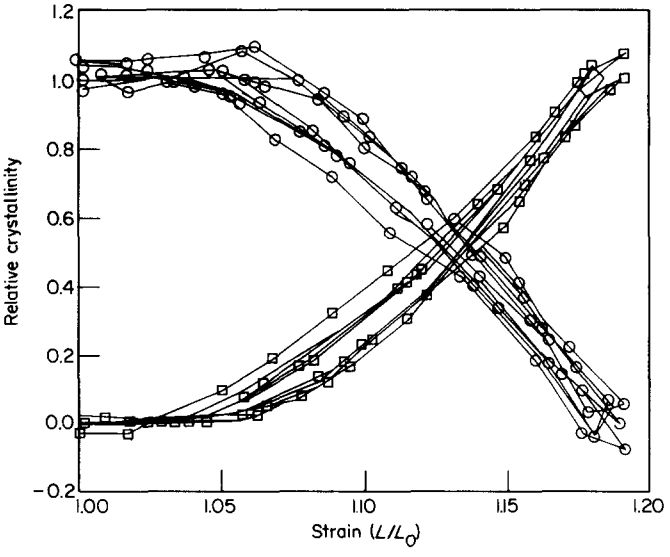

Figure 12 Relative α (○) and β (X) crystallinity as a function of strain based on least squares fit of 1000–900 cm^{-1}

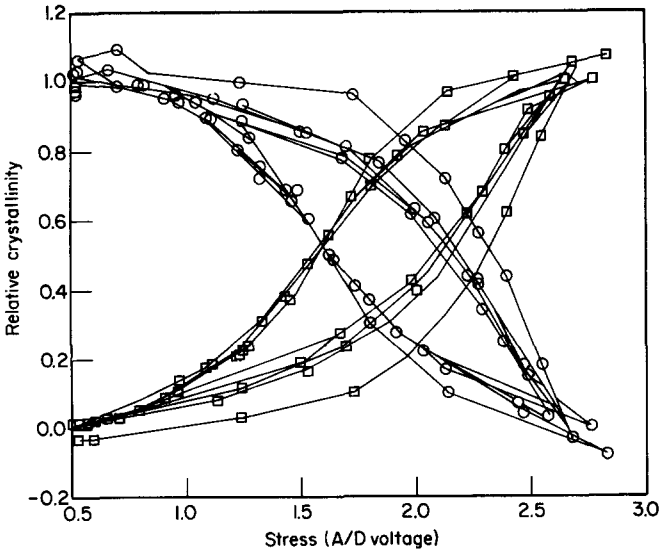

Figure 13 Relative α (O) and β (X) crystallinity as a function of stress A/D voltage on least squares fit of 1000–900 cm^{-1}

It must be remembered, however, that although the discussion thus far has focused primarily on the α to β transition, the amorphous phase will obviously play a significant role in dictating the mechanical properties of the sample. One interpretation of these results is that the phase transition from α to β is essentially an elastic phenomenon, whereas the amorphous phase is deformed via a viscoelastic mechanism. These results are in complete agreement with those proposed recently by Strohmeier and Frank[42]. They suggest that the mechanical behaviour can be modelled with the α→β phase transition represented as a Hookean spring in series with a Voigt–Kelvin element representing the viscoelastic amorphous component.

CONCLUSIONS

Fast scan time resolved infra-red studies of the α→β crystal:crystal phase transition in PTMT have confirmed the reversibility of the transition after the first deformation cycle. In contrast to another infra-red investigation, a number of conformationally sensitive vibrational modes have been shown to revert to their original intensities when the strain is relieved. Factor analysis of 2 conformationally sensitive regions using spectra collected over the course of a single deformation cycle indicates the presence of 2 pure components: i.e. the α and β crystal phases. Although the molecules within the amorphous phase are most likely undergoing some conformational changes, it is clear that such modifications do not involve transitions to either of the crystal phases. Spectral least squares curvefitting indicates that above strains of ~5% the transition from α to β is directly proportional to the applied strain in an almost completely reversible fashion. The data presented support an earlier mechanical model which postulates that the crystalline domains can be described as a Hookean element in series with a Voigt–Kelvin viscoelastic element corresponding to the amorphous phase.

ACKNOWLEDGEMENT

The authors wish to thank the National Science Foundation for their support of this paper through the Materials Research Laboratory of Case Western Reserve University under Grant No. DMR81-19425.

REFERENCES

1 Boye, C. A. and Overton, J. R. *Bull. Am. Phys. Soc., Ser. 2*, 1974, **19**, 352
2 Poulin-Dandurand, S., Perez, S., Revol, J.-F. and Brisse, F. *Polymer* 1979, **20**, 419
3 Brisse, F., Marchessault, R. H. and Perez, S. 'Preparation and Properties of Stereoregular Polymers', D. Reidel Pub., 1979, p. 407
4 Hall, I. H. and Ibrahim, B. A. *Polymer* 1982, **23**, 805
5 Noah, J. and Prud'Homme, R. E. *Eur. Polym. J.* 1980, **16**, 1027
6 Roche, E. J., Stein, R. S. and Thomas, E. L. *J. Polym. Sci., Polym. Phys. Edn.* 1980, **18**, 1145
7 Yokouchi, M., Sakakibara, Y., Chatani, Y., Tadokoro, H., Tanaka, T. and Yoda, K. *Macromolecules* 1976, **9**, 266
8 Stambaugh, B. D., Koenig, J. L. and Lando, J. B. *J. Polym. Sci., Polym. Phys. Edn.* 1979, **17**, 1053
9 Hall, I. H. and Pass, M. G. *Polymer* 1976, **17**, 807
10 Alter, U. and Bonart, R. *Colloid Polym. Sci.* 1976, **254**, 348
11 Desborough, I. J. and Hall, I. H. *Polymer* 1977, **18**, 825
12 Joly, A. M., Nemoz, G. and Georges Vallet, A. D. *Makromol. Chem.* 1975, **176**, 479
13 Hall, I. H. *ACS Symposium Series* **141**, 346
14 Mencik, Z. *J. Polym. Sci.* 1975, **13**, 2173
15 Bonart, R. and Schultze-Gebhardt, F. *Ang. Makromol. Chem.* 1972, **22**, 41
16 Jakeways, R., Ward, I. M., Wilding, M. A., Hall, I. H., Desborough, I. J. and Pass, M. G. *J. Polym. Sci., Polym. Phys. Edn.* 1975, **13**, 799
17 Davidson, I. S., Manuel, A. J. and Ward, I. M. *Polymer* 1983, **24**, 30
18 Jelinski, L. W., Dumais, J. J. and Engel, A. K. Seattle ACS
19 Jelinski, L. W. and Dumais, J. J. *Macromolecules* (submitted)
20 Jelinski, L. W., Dumais, J. J., Watnick, P. I., Engel, A. K. and Sefcik, M. D. *Macromolecules* (submitted)
21 Jelinski, L. W., Dumais, J. J. and Engel, A. K. *Macromolecules* (submitted)
22 Jelinski, L. W. *Macromolecules* 1981, **14**, 1341
23 Ward, I. M. and Wilding, M. A. *Polymer* 1977, **18**, 327
24 Siesler, H. W. (to be published)
25 Stambaugh, B. D., Koenig, J. L. and Lando, J. B. *J. Polym. Sci., Polym. Lett. Edn.* 1977, **15**, 299
26 Siesler, H. W. *Polym. Prepr.* 1980, **21**, 163
27 Siesler, H. W. *Makromol. Chem.* 1979, **180**, 2261
28 Siesler, H. W. *J. Polym. Sci., Polym. Lett. Edn.* 1979, **17**, 453
29 Holland-Moritz, K. and Siesler, H. W. *Polym. Bull.* 1981, **4**, 165
30 Stambaugh, B. D., Lando, J. B. and Koeing, J. L. *J. Polym. Sci.* 1979, **17**, 1063
31 Stach, W. and Holland-Moritz, K. *J. Mol. Struct.* 1980, **60**, 49
32 Seisler, H. W. personal communication
33 Holland-Moritz, K., Stach, W. and Holland-Moritz, I. *Progr. Colloid Polym. Sci.* 1980, **67**, 161
34 Stach, W. *Doktor Dissertation*, Instituet fuer Physikalische Chemie, Universitaet Koeln, Koeln, West Germany
35 Siesler, H. W. *J. Mol. Struct.* 1980, **59**, 15
36 Stockr, J., Schneider, B., Doskocilova, D., Loevy, J. and Sedlacek, P. *Polymer* 1982, **23**, 714
37 Stach, W. W. and Holland-Moritz, K. H. IUPAC Proc. of 28th Macromol. Symp., Amherst, Mass., 12–16 July 1982
38 Boerio, F. J., Bahl, S. K. and McGraw, G. E. *J. Polym. Sci.* 1976, **14**, 1029
39 Jakeways, R., Smith, T., Ward, I. M. and Wilding, M. A. *J. Polym. Sci., Polym. Lett. Edn.* 1976, **14**, 41
40 Brereton, M. G., Davies, G. R., Jakeways, R., Smith, T. and Ward, I. M. *Polymer* 1978, **19**, 17
41 Alter, U. and Bonart, R. *Colloid Polym. Sci.* 1980, **258**, 332
42 Strohmeier, W. and Frank, W. F. X. *Macromolecules* 1980, **13**, 137